SINTECHCOM: Science, Technology and Communication Journal
Vol. 2, No. 3, June 2022, pp. 91-96, DOI: 10.59190/stc.v2i3.215

Inspection of birefringence characteristics to establish single-mode fiber quality

Yoli Zairmi[1,*], Doni Basdyo[1], Haryana Mohd Hairi[2], Muhammad Safwan Abd Aziz[3], Hewa Yaseen Abdullah[4,5]
[1]Department of Physics, Universitas Riau, Pekanbaru 28293, Indonesia
[2]Department of Physics, Universiti Teknologi MARA, Shah Alam 40450, Malaysia
[3]Department of Physics, Universiti Teknologi Malaysia, Johor 81310, Malaysia
[4]Research Center, Salahaddin University, Erbil 44002, Iraq
[5]Department of Physics Education, Tishk International University, Erbil 44001, Iraq

ABSTRACT

Birefringence characterization has been carried out for single-mode fiber (SMF) consisting of SMF-28, SMF-28e, SMF-28e+, SMF-28e+LL, and SMF-28ULL. The parameters that were varied were the refractive index of the core and the cladding, while the radii of both were equal to the wavelength of 1550 nm. Birefringence characterized by simulation can determine the quality of SMF by knowing the changes in the light propagation constant caused by polarized light on optical fibers. The simulation results show that in SMF-28ULL there is a propagation constant or birefringence which has a large influence compared to other types of SMF such as the magnitude of polarization and reducing power.

ARTICLE INFO

Article history:

Received May 13, 2022
Revised May 28, 2022
Accepted Jun 9, 2022

Keywords:

Birefringence
Polarization
Propagation
Single-Mode Fiber
Wavelength

* **Corresponding Author**
E-mail address: yoli.zairmi@student.unri.ac.id

1. INTRODUCTION

The use of copper cables as a transmission medium in communication systems is no longer capable of transmitting long-distance data with large capacity and high speed because of a lot of noise and small bandwidth [1-3]. Therefore, the use of copper cable as a transmission medium is replaced by fiber optics with higher capabilities [4, 5].

Optical communication systems have been around since the 1700s, beginning with the invention of the optical telegram by a French engineer named Claude Chappe [6-8]. Advances in optical fiber to date have prompted Corning Incorporated to develop single-mode fiber (SMF) with attenuation below 20 dB/km [9, 10]. SMF has the advantage of several criteria such as range, functionality, sensitivity and accuracy [11-13]. SMF can be used as a coupler in an optical system that functions as a link in combining and splitting optical signals as an optical switch [14, 15].

SMF has a large transmission bandwidth which can be applied in long-distance communication [16-18]. This type of optical fiber has high data transfer capabilities due to the absence of modal noise, low attenuation, compatibility with integrated optical technology and is durable [19, 20]. SMF devices usually use thin films in the manufacture of their components because they have a high mass density and a good modulus of elasticity so they are not easily broken [21-23]. This fabrication gives SMF properties as a light wave power transmission that is superior to other media. In addition, SMF also has various characteristics based on the propagation constant or birefringence it

produces [24, 25]. It is therefore important to review the birefringence characteristics to determine the quality of the SMF from the effects of power reduction and polarization changes by imperfect cylindrical fiber cores.

2. RESEARCH METHODS

The types of SMF used are SMF-28, SMF-28e, SMF-28e+, SMF-28e+LL, and SMF-28ULL. The initial step in the birefringence characterization is to determine the SMF profile using the core and cladding parameters with a diameter of 4.1 μm and 62.5 μm, while the refractive index profile of each type of SMF can be seen in Table 1.

Table 1. Refractive index of core and cladding of each type of SMF.

SMF type	Core	Cladding
SMF-28	1.45213	1.44692
SMF-28e	1.46770	1.46240
SMF-28e+	1.45173	1.44602
SMF-28e+LL	1.45223	1.44702
SMF-28ULL	1.44525	1.44002

The birefringence characterization process is carried out in a simulation by determining the SMF profile using a refractive index profile type with regions 0 and 1. The input parameter is the core 0 region while the output is the cladding region 1. The SMF constituent materials used are pure silica, germanium as a positive dopant, and fluorine as a negative dopant. SMF birefringence simulation using LP mode (matrix method) was carried out to generate the index and modal fiber field at certain wavelengths. The cut-off navigator menu with LP mode aims to display the cut-off wavelength parameters for the LP01 and LP11 optical fiber modes. Fundamental mode property simulation is done by determining the default parameter values for material, bending, and loss parameters. In the scan section, the wavelength is adjusted to the default option, while in the parameter section values are entered from 1.2 to 1.6 with 100 iterations. The birefringence simulation due to parameter disturbance begins by determining the photoelastic fiber constant of 3.44 × 1011 m^2/kgW, Young's modulus of 775 × 10^7 kgW/m^2, and Poisson ratio. The flexural factor and extrinsic stress in SMF also affect the birefringence simulation. The value used in SMF bending is 0.12 m with a circular fiber tensile force of 0.5 N. At the output, the spectral range is set at 0.4 μm with 51 iterations.

Birefringence is defined as the difference between the propagation constants of the eigenmode polarizations shown in the following equation [26-28]:

$$\Delta\beta = \beta_x - \beta_y \tag{1}$$

Birefringence caused by lateral stress is as follows:

$$\Delta\beta_{lateral\ stress} = -8\frac{Cpk_0}{\pi d}\left[1 - \left(\frac{a}{d}\right)^2 H(V)\right] \tag{2}$$

The birefringence caused by bending is as follows:

$$\Delta\beta_{bending} = -\frac{1}{8}\left(\frac{d}{R}\right)^2 ECk_0\left[1 - \frac{1}{3}\left(\frac{a}{d}\right)^2 H(V)\right] \tag{3}$$

The birefringence caused by the voltage is as follows:

$$\Delta\beta_{tension-coiled} = -2\frac{2-3v}{1-v} C\frac{f}{\pi dRc}k_0 \tag{4}$$

$$H(V) = 2 + \frac{4(U^2 - W^2)}{U^2V^2W^2} + \frac{4}{U}\frac{J_0(U)}{J_1(U)} \tag{5}$$

$$U = a\sqrt{n_1^2 k_o^2 - \beta^2} \tag{6}$$

$$W = a\sqrt{\beta^2 - n_2^2 k_o^2} \tag{7}$$

$$V = \frac{2\pi a}{\lambda}(n_1{}^2 - n_2{}^2)^{\frac{1}{2}} \tag{8}$$

3. RESULTS AND DISCUSSIONS

The original optical fiber does not have a perfect cylindrical core but there is a variation in diameter that causes non-uniform stresses along the optical fiber so that the constant propagation of the two polarizing components is different and the fiber becomes birefringence. Linearly polarized light is fed to the SMF assuming that the two polarized components have the same amplitude and there is no phase difference at the output end, but as the light propagates along the fiber, one mode is out of phase in the other due to the difference in the phase propagation constant. So at any point along the fiber (for random phase differences) the two components will produce elliptically polarized light. At the $\pi/2$ phase difference, circularly polarized light will be generated. In this way the polarization progresses from linear to elliptical to circular to elliptical and back to linear. This alternating polarization continues along the fiber [26, 29].

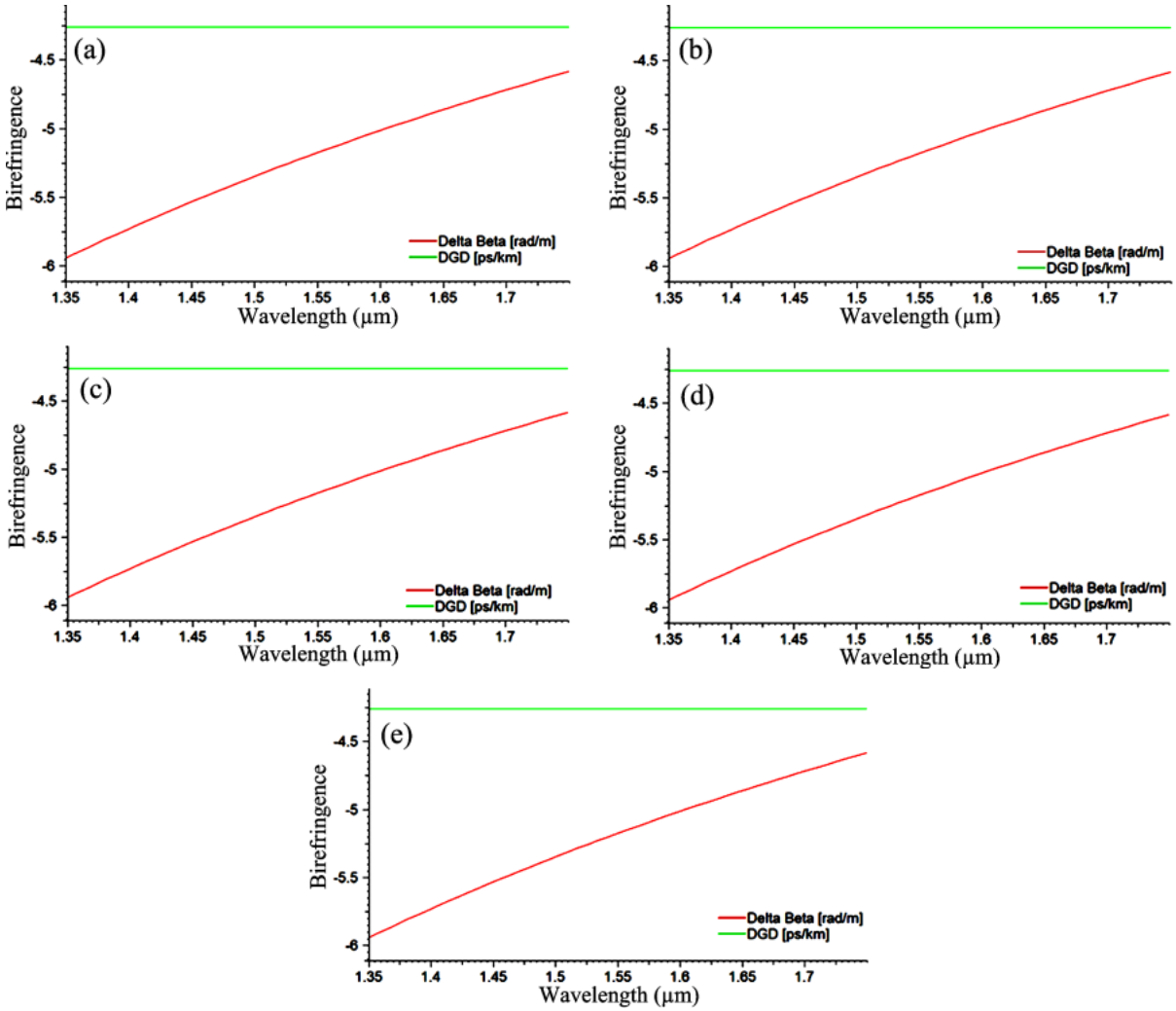

Figure 1. Birefringence results for (a) SMF-28, (b) SMF-28e, (c) SMF-28e+, (d) SMF-28e+LL, and (e) SMF-28ULL.

Birefringence can be caused by intrinsic and extrinsic factors, intrinsic interference occurs accidentally in the manufacturing process and is a permanent feature of optical fibers. These include noncircular cores and asymmetric stress fields in the fibers around the core region. Non-circular nuclei give rise to geometric birefringence, whereas non-symmetrical stress fields create stress birefringence. Birefringence can also be created in the fiber when subjected to an external force on the handle or cable. Extrinsic factor birefringence is caused by lateral pressure, bending, and twisting. These three mechanisms are usually present to some extent in fiber optic telecommunications [30-32].

Simulation of birefringence caused by extrinsic factors, namely bending force and stress were kept constant in all types of SMF to see the effect of intrinsic factor. The birefringence that occurs in SMF-28, SMF-28e, SMF-28e+, SMF-28e+LL, and SMF-28ULL is shown in Figure 1.

The birefringence increases with increasing wavelength due to the polarization difference of the second phase, whereas the addition of the delay group (DGD) results in an increase in the difference in wavelength. The magnitude of the birefringence at a wavelength of 1550 nm for the optical fiber SMF-28 is -5.1753668 rad/m, SMF-28e is -5.17534 rad/m, SMF-28e+ is -5.17539 rad/m, SMF-28e+LL is -5.14879 rad/m, and SMF-28eULL is -5.175397 rad/m. In SMF-28ULL the birefringence value is greater than in other fibers which shows a large reduction in output power. Polarized light in SMF is a magnetic field and an electric field.

The greater the Birefringence value or the difference in the wave propagation constant, the more polarization occurs in the optical fiber. The phase difference between the magnetic field and the electric field becomes larger with the optical fiber core not perfectly circular due to the bending and stress forces when the fiber is coiled. In the simulation results with the same extrinsic birefringence parameters used for all, the birefringence values are different because of the different modes of each type of SMF and the refractive index of the core and cladding used.

4. CONCLUSION

Birefringence that occurs in optical fiber is influenced by external factors caused by bending and stress forces. This factor makes the fiber optic core no longer circular but changes shape to an ellipse. Light waves will undergo elliptical or circular polarization, resulting in two waves that have different phases. In SMF-28ULL the large birefringence value indicates that there is a lot of polarization and power reduction, while the SMF-28e+LL has birefringence with the smallest impact.

ACKNOWLEDGMENTS

The authors would like to thank the Ministry of Education and Culture of the Republic of Indonesia which has funded research through the 2022 DRTPM program, as well as the University of Riau Research and Community Service Institute (LPPM) which has partially supported this research through a 2022 grant.

REFERENCES

[1] Mahmood, S. H. & Salih, A. M. (2019). Study of the most important factors affecting on efficiency of power line communication systems. *Journal of Engineering and Sustainable Development*, **23**(5), 55–70.

[2] Erlinda, S., Veriyanti, V., & Saktioto, T. (2022). The effect of light waves on polarization mode disperts. *Science, Technology and Communication Journal*, **2**(2), 49–54.

[3] Veriyanti, V., & Saktioto, S. (2020). Tampilan birefringence pada gangguan pembengkokan serat optik komersial. *Indonesian Physics Communication*, **17**(2), 97–103.

[4] Nyarko-Boateng, O., Xedagbui, F. E. B., Adekoya, A. F., & Weyori, B. A. (2020). Fiber optic deployment challenges and their management in a developing country: A tutorial and case study in Ghana. *Engineering Reports*, **2**(2), e12121.

[5] Qarkaxhija, J. (2018). Optic Fibers as a Broadcasting Media. *Prizren Social Science Journal*, **2**(1), 1–13.

[6] Garfinkel, S. L. & Grunspan, R. H. (2019). *The computer book: From the abacus to artificial intelligence, 250 milestones in the history of computer science*. Union Square & Co.

[7] Oppitz, M. & Tomsu, P. (2018). *Early information network services*. Inventing the Cloud Century-Springer, 45–73.

[8] Homer, T. (2012). *The Book of Origins: The first of everything-from art to zoos*. Hachette UK.
[9] Sakr, H., Chen, Y., Jasion, G. T., Bradley, T. D., Hayes, J. R., Mulvad, H. C. H., Davidson, I. A., Numkam Fokoua, E., & Poletti, F. (2020). Hollow core optical fibres with comparable attenuation to silica fibres between 600 and 1100 nm. *Nature Communications*, **11**(1), 1–10.
[10] Erlinda, S. & Saktioto, S. (2020). Pengaruh spektra gelombang cahaya terhadap dispersi moda polarisasi. *Seminar Nasional Fisika Universitas Riau V (SNFUR-5)*, **5**(1), 1–5.
[11] Tahir, B. A., Ali, J., Saktioto, Fadhali, M., Rahman, R. A., & Ahmed, A. (2008). A study of FBG sensor and electrical strain gauge for strain measurements. *Journal of Optoelectronics and Advanced Materials*, **10**(10), 2564–2568.
[12] Azizah, Y. N., Hairi, H. M., & Candra, W. (2022). Characteristics of fiber Bragg grating due to temperature changes in honey solution. *Science, Technology and Communication Journal*, **2**(2), 63-68.
[13] Saktioto, Rahmat, I., & Juandi. (2016). Penentuan rugi-rugi kelengkungan fiber optik mode tunggal secara komputasi. *Indonesian Physics Communication*, **13**(13), 896–900.
[14] Saktioto, Ali, J., Fadhali, M., Rahman, R. A., & Zainal, J. (2008). Modeling of coupling coefficient as a function of coupling ratio. *Ninth International Symposium on Laser Metrology*, **7155**, 558–567.
[15] Azizah. Y. N. & Saktioto, S. (2020). Karakteristik perubahan temperatur beberapa madu kemasan menggunakan fiber Bragg grating (FBG). *Seminar Nasional Fisika Universitas Riau V (SNFUR-5)*, **5**(1), 1–6.
[16] Rademacher, G., Luis, R. S., Puttnam, B. J., Eriksson, T. A., Ryf, R., Agrell, E., Maruyama, R., Aikawa, K., Awaji, Y., Furukawa, H., & Wada, N. (2019). High capacity transmission with few-mode fibers. *Journal of Lightwave Technology*, **37**(2), 425–432.
[17] Poggiolini, P. & Poletti, F. (2022). Opportunities and challenges for long-distance transmission in hollow-core fibres. *Journal of Lightwave Technology*, **40**(6), 1605–1616.
[18] Abdullah, M. F. L., Omar, K. A., Qasim, A. A., Abdulrahman, A. M., & Dawood, A. (2019, March). Radio over fiber (RoF) implementation using MZM for long distance communication. *2019 international conference on information science and communication technology (ICISCT)*, 1–6.
[19] Francesca, D. D., Vecchi, G. L., Girard, S., Morana, A., Reghioua, I., Alessi, A., Hoehr, C., Robin, T., Kadi, Y., & Brugger, M. (2019). Qualification and calibration of single-mode phosphosilicate optical fiber for dosimetry at CERN. *Journal of Lightwave Technology*, **37**(18), 4643-4649.
[20] Fitri, A., Candra, W., & Meyzia, B. (2021). Determination of optical parameters on knee bending of the feet using fiber optic. *Science, Technology and Communication Journal*, **2**(1), 9-14.
[21] Chaudhary, K. T., Qindeel, R., Saktioto, Hussain, M. S., Ali, J., & Yupapin, P. P. (2011). Graphite thin film deposition using laser induced plasma. *Procedia Engineering*, **8**, 423–427.
[22] Zhang, H., Huang, T., Jiang, Q., He, L., Bismarck, A., & Hu, Q. (2021). Recent progress of 3D printed continuous fiber reinforced polymer composites based on fused deposition modeling: a review. *Journal of Materials Science*, **56**(23), 12999–13022.
[23] Kabir, S. F., Mathur, K., & Seyam, A. F. M. (2020). A critical review on 3D printed continuous fiber-reinforced composites: History, mechanism, materials and properties. *Composite Structures*, **232**, 111476.
[24] Zainuddin, N. A. A. M., Ariannejad, M. M., Arasu, P. T., Harun, S. W., & Zakaria, R. (2019). Investigation of cladding thicknesses on silver SPR based side-polished optical fiber refractive-index sensor. *Results in Physics*, **13**, 102255.
[25] Zhao, Q., Liu, J., Yang, H., Liu, H., Zeng, G., & Huang, B. (2022). High birefringence D-shaped germanium-doped photonic crystal fiber sensor. *Micromachines*, **13**(6), 826.
[26] Sakai, J. I. & Kimura, T. (1981). Birefringence and polarization characteristics of single-mode optical fibers under elastic deformations. *IEEE Journal of Quantum Electronics*, **17**(6), 1041–1051.
[27] Saktioto, Zairmi, Y., Veriyanti, V., Candra, W., Syahputra, R. F., Soerbakti, Y., Asyana, V., Irawan, D., Okfalisa, Hairi, H., Hussein, N. A., Syamsudhuha, & Anita, S. (2020, October). Birefringence and polarization mode dispersion phenomena of commercial optical fiber in

telecommunication networks. In *Journal of Physics: Conference Series* (Vol. 1655, No. 1, p. 012160). IOP Publishing.

[28] Fördös, T., Jaffrès, H., Postava, K., Seghilani, M. S., Garnache, A., Pištora, J., & Drouhin, H. J. (2017). Eigenmodes of spin vertical-cavity surface-emitting lasers with local linear birefringence and gain dichroism. *Physical Review A*, **96**(4), 043828.

[29] Zhao, H. & Li, H. (2021). Advances on mode-coupling theories, fabrication techniques, and applications of the helical long-period fiber gratings: A review. *Photonics*, **8**(4), 106.

[30] Poole, C. D. & Nagel, J. (1997). Polarization effects in lightwave systems. *Optical Fiber Telecommunications IIIA*, 114–161.

[31] Hao, P., Yu, C., Feng, T., Zhang, Z., Qin, M., Zhao, X., He, H., & Yao, X. S. (2020). PM fiber based sensing tapes with automated 45° birefringence axis alignment for distributed force/pressure sensing. *Optics Express*, **28**(13), 18829–18842.

[32] Budinski, V., & Donlagic, D. (2017). Fiber-optic sensors for measurements of torsion, twist and rotation: A review. *Sensors*, **17**(3), 443.